Prevention of the Ground Subsidence by using the Foot Reinforcement Side Pile during the Shallow Overburden Tunnel Excavation in Unconsolidated Ground

Ying Cui[*], Kiyoshi Kishida[2] and Makoto Kimura[3]

1 Department of Civil Engineering, Meijo University, Nagoya 468-5802, JAPAN

2 Department of Urban Management, Kyoto University, Kyoto 615-8540, JAPAN

3 Department of Civil and Earth Resources Engineering, Kyoto University, Kyoto 615-8540, JAPAN

*Corresponding author: cuiying@meijo-u.ac.jp; Tel: +81-52-838-2346

Abstract

Large settlements of the ground surface, crown and foot of a tunnel have been measured at a construction field that an NATM tunnel has been excavated under shallow overburden and unconsolidated ground conditions. For these settlements, it was assumed that if the settlement at the foot of the tunnel had been prevented, the ground subsidence can be controlled effectively. Based on this idea, Foot Reinforcement Side Pile (FRSP) has been utilized to prevent the ground settlement. It was reported that the FRSP could effectively prevent the settlements of ground surface and tunnel during the construction period. However, the mechanism of how the FRSP prevents the settlements of tunnel and surrounding ground has not been clearly understood. In practice, several parameters of the FRSP, such as the length, the spacing and the diameter of the pile, have been determined through the practical construction works.

In this paper, three dimensional trapdoor model experiments and the corresponding numerical analyses, and numerical analyses for the actual tunnel excavation are carried out to examine the effect of FRSP on preventing settlements of ground surface and crown and foot of tunnel, and to discuss its mechanism. As a result, it was observed that the FRSP can prevent settlements of the ground surface and tunnel effectively, and these effects of the FRSP are connected with the distance from the tunnel lining to the slip line. When the FRSP is long enough to cross the shear line, it can exert the effect of the shear reinforcement, load redistribution and internal pressure to prevent the settlements of the tunnel and surrounding ground effectively.

KEYWORDS: foot reinforcement side pile, tunnel excavation, shallow overburden, unconsolidated ground, settlement, trapdoor

1. Introduction

Up to now, cut and cover method has been widely used as the main tunneling method for excavating a shallow overburden tunnel in soft ground. Recently, due to the development of the construction and measurement techniques, the construction of the shallow overburden tunnel in soft ground using New Austrian Tunneling Method (NATM) have been increasing (Yokoyama et al., 1987; Kitagawa et al., 2004; Irshad and Heflin, 1988; Akutagawa et al., 2006; Pinto et al, 2013). However, since the unconsolidated ground has the low stiffness and the ground arch action is not effective enough due to the shallow overburden, large ground subsidence frequently occurs in the construction field (Fukushima et al, 1989; Adachi et al, 1986). For example, due to the topography and route conditions, a shallow overburden tunnel on unconsolidated ground using NATM was excavated during the construction of a new bullet train line in Japan and various auxiliary tunneling methods were applied in order to ensure the safety of the construction (Miwa and Ogasawara, 2005). In this construction field, the large settlements of the ground surface, crown and foot of the tunnel have been measured as shown in **Figure 1 (a)** (Kitagawa et al., 2009), and these settlements show almost the same value. This phenomenon was called an accompanied settlement, and the prevention of ground, crown and face of tunnel has become an important issue.

For the phenomenon of the accompanied settlement, it was assumed that the ground subsidence can be effectively prevented, if the settlement at the foot of tunnel had been prevented. Based on this idea, Foot Reinforcement Side Piles (FRSP) had been utilized in the construction site as shown in **Figure 2**. The FRSP is one of the foot reinforcement methods, which is performed by inserting a steel pile into the ground from the inside of the tunnel, and it was reported that the FRSP can effectively prevent the settlement in the shallow overburden and unconsolidated construction conditions. The temporal changes in the settlements of the abovementioned tunnel and the convergence, which were measured in the mentioned field are shown in **Figure 1**. The settlements measured in the field without FRSP and with FRSP installed are shown in **Figure 1 (a)** and **Figure 1 (b)** respectively (Kitagawa et al., 2009). The comparison of these figures indicates that the settlements of both crown and foot of the tunnel became smaller by installing the FRSP. However, even though the effects of the FRSP have been reported in the field, the mechanism of how the FRSP preventing the settlements is still not clearly understood. In practice, several parameters of the FRSP, such as the length, the spacing, the diameter and the position of the pile, has been determined through the

practical construction works. Therefore, there is a need for the clarification of the applying method of the FRSP.

On the other hand, several auxiliary methods have been developed with the increasing of the construction fields of tunnels under shallow overburden and unconsolidated conditions, and many researches have been carried out for the shallow tunnels and auxiliary methods. A variety of model experiments and numerical analyses were performed to investigate the mechanical behavior of shallow tunnels, which were excavated under unconsolidated ground conditions. Shimada (1980) carried out a series of model experiments to investigate the mechanism of the surface settlement during shallow tunnel excavation. Moreover, Finite Element (FE) simulations have been performed by Akutagawa et al. (2006) to predict the ground movement caused by tunneling of a shallow NATM tunnel in unconsolidated soil. On the other hand, some auxiliary methods, such as forepoling (Fukushima et al, 1989), umbrella arch method (Ocak, 2008; Yoo and Shin, 2003), footing reinforcement bolt and pile (Fang et al, 2012) and pipe roof (Okawa et al., 1985; Fang et al, 2012) are widely used when excavating a shallow tunnel under unconsolidated constructions, and the effect of these methods have been described in the literature.

For the effect of the FRSP, Kitagawa, et al. (2009, 2010) carried out a series of model experiments (Kitagawa, et al., 2009) and corresponding rigid-plastic FE analysis (Kitagawa, et al., 2010) to concerning the effects of the FRSP on preventing surface settlement. The experimental and numerical results showed that, the FRSP were effective on preventing ground settlement when they were long enough to intersect with the slip line, and the effects increased with the FRSP became longer. Moreover, the FRSP became more effective, when (i) it was fixed to the tunnel tightly, (ii) the ground had large internal friction angle, and (iii) it was installed at the lower part of the tunnel. In this research, the footing of the tunnel was modelled as a T shaped model and the lining model are rotating with the descending of the trapdoor. However, the T shaped section is different with the shape of the real tunnel footing; furthermore, the rotation of the tunnel footing has not been measured in the field. Therefore, it is thought that the T shaped footing model cannot represent the mechanical behavior of the real tunnel lining appropriately. On the other hand, the rigid plastic finite method can only be used to discuss the limit state of the soil, and it cannot consider the mechanical behavior of the ground and the FRSP during the tunnel excavation process. Moreover, the influence of the parameters such as the length of the FRSP, and the mechanism of the

FRSP's effect were not discussed in detail.

Hence, in this study, three dimensional trapdoor experiments, corresponding numerical analyses and the numerical analyses for actual tunnel work are performed in order to discuss the mechanism of the effect of the FRSP. First of all, the model of the tunnel footing is improved based on the abovementioned literature (Kitagawa, et al., 2009), and a series of three dimensional trapdoor model experiments and corresponding elasto-plasticity FE analyses are carried out to define the effect of the FRSP more clearly. Moreover, the tunnel excavation processes in the real field are simulated by using the elasto-plasticity FE method, to investigate the mechanical behavior of the ground and the FRSP during the tunnel excavation process for clearly defining the mechanism of the effect of the FRSP.

2. Layout of model experiments and analyses

2.1 Three-dimensional trapdoor model experiments

In order to consider the effect of the FRSP and the influence of the length of FRSP, a series of model experiments were carried out with different length of the FRSP. **Figure 3** shows the schematic diagram of the experiment apparatus used in the model experiments, namely three dimensional (3D) trapdoor apparatus. The tunnel excavation process was simulated with lowering a supporting plate, which is called a trapdoor. The trapdoor experiment apparatus are adopted to investigate the mechanism of tunnel excavation problems by many researchers in the past (e.g. Murayama and Matsuoka, 1971; Nakai et al., 1997; Adachi et al., 2003).

The displacement of the trapdoor and the vertical load acting on the bottom of the chamber have been measured in all of the lowering processes. Displacement of the trapdoor was measured by a contact displacement transducer which installed in the lower part of the trapdoor. The measuring range of this displacement transducer is 25 mm and its sensitivity is 500 μ strain/mm. Moreover, Three pieces of load measurement plates (Trapdoor, Panel A and Panel B) were installed at the bottom of the chamber to measure the load that was acting on these plates. The measuring range of the load cell is 50 kN and its resolution is 0.1599～0.6493 N/μ strain. Moreover, Shape of the ground surface was measured before lowering trapdoor and when the trapdoor is lowered to 0.5, 1, 2, and 3 mm. The settlement of the ground

surface was determined as the difference of the shape of ground surface from the initial shape. Shape of ground surface was measured by a surface monitoring system, which was installed above the model ground as shown in **Figure 3**. An laser sensor which can move in the horizontal direction at a prescribed speed along the driving rail, was installed in the surface monitoring system, to measure the shape of the ground surface. The measuring range of the sensor for the vertical displacement is plus and minus 5mm, and the resolution is 2μm.

The model ground was prepared by the air pluviation of the dried Toyoura silica sand from 600 mm height above the ground surface. The properties of the model ground are listed in **Table 1.** In this experiment, the footing of the tunnel was modeled as L-shaped, with details shown in **Figure 3**. It was made of aluminum and 5 circular holes have been created for installing the FRSP model. The FRSP was modeled by wood piles that were 5 mm in diameter and the piles were fixed rigidly on the tunnel lining model. The Young's modulus of the FRSP model was 14.2×10^6 kN/m^2.

2.2 Numerical analyses of the model experiment

In order to describe more clearly the mechanical behavior of the FRSP and the surrounding ground when lowering the trapdoor, the numerical analysis of the model experiment was executed by using 3D elasto-plasticity FE method. The analysis mesh and boundary conditions are shown in **Figure 4**. Due to the symmetrical condition of the ground, only half of the width in y direction was considered. The lowering of the trapdoor is modeled by applying the prescribed vertical displacement to the nodes located on the trapdoor. Considering the theory of infinitesimal deformation, 2 mm displacement was given to the mentioned nodes which is smaller than 3 mm deformation that was applied to the trapdoor during the experiment. In addition, for the right edge of trapdoor which displaced discontinuously during the lowering process of trapdoor, a gradient was given to the displacement of the boundary nodes (Kikumoto et al., 2003) as shown in **Figure 4(b)**.

FE analysis code DBLEAVES (Ye et al., 2007) was employed in this study. An elasto-plastic constitutive model named *Subloading t_{ij} model* (Nakai and Hinokio, 2004) was used to simulate the mechanical properties of the ground material. This constitutive model can properly describe the influences of the intermediate principal stress, the dependence of the direction of plastic flow on the stress paths, density and

the confining pressure on the deformation and strength of soils. The parameters used in this numerical analyses are listed in **Table 2**(Cui et al., 2007).

Hybrid element model proposed by Zhang et al. (2000) was used to simulate the FRSP. The hybrid element model is composed of the elastic solid elements and a beam element, with the beam element surrounded by the column elements. Solid elements can express the influence of the volume of the FRSP. The stiffness of the pile is shared by the beam element and several solid elements in such a way that the bending stiffness of the pile *EI* is equal to the sum of the bending stiffness of the beam element $(EI)_{beam}$ and solid elements $(EI)_{solid}$. The sharing ratio between the stiffness of the beam element and the solid elements is determined as 9 to 1, by refer to the previous study (Zhang, et al., 2000). The Young's Modulus of the beam element and solid element that were calculated by using the above mentioned method are 13.5×10^6 kN/m^2 and 6.65×10^5 kN/m^2 respectively.

Figure 5 shows the surface settlement profiles due to the lowering the trapdoor to 0.5, 1.0 and 2.0 mm, for the case no FRSP was installed. **Figure 5 (a)** was obtained from the experiments when the **Figure 5 (b)** was obtained from corresponding numerical analyses. Numerical results, particularly for the lowering displacement of 0.5 and 1.0 mm, show a good agreement with the experiment. Hence, it can be said that the numerical analysis conducted in this study can simulate the mechanical behavior of the ground due to the lowering of the trapdoor appropriately.

3. Discussion on model experiments and corresponding analyses

3.1 Effect of FRSP on preventing surface settlement

The surface settlement profiles measured in the model experiment for the cases without the FRSP and with 200 mm long FRSP model have been installed at the time of the trapdoor was lowered to 3 mm are shown in **Figure 6 (a)**. It is observed from the figure that the surface settlement becomes smaller by installing the FRSP. The maximum surface settlement and the volume of the settlement trough (Mair et al., 1993) are used for evaluating the effect of FRSP. The maximum surface settlement has occurred on the boundary between the lining model and the ground. The volume of the settlement trough is the area between the x-axis and the curve, which is marked as the shaded region in **Figure 6 (a)**. The volume of the

settlement trough shows the overall level of the surface settlement in the shaded area. **Figure 6 (b)** shows the reduction ratios of the maximum surface settlement and the volume of the settlement trough obtained from model experiments and numerical analyses when the FRSP with different lengths was installed. The x-axis represents the length of the FRSP model. The results of both experiments and numerical analyses indicate that the FRSP is effective when it is longer than 100 mm, when FRSP is almost no effect when it is shorter than 100 mm. The FRSP becomes more effective with the increase in its length and this effect becomes stable when the FRSP is longer than 260 mm. In addition, the numerical results denote the same tendency as the model experiment. Hence, it can be suggested that the numerical analysis can successfully simulate the mechanical behavior of the ground and the FRSP in model experiment.

In **Figure 7 (a)**, the vertical earth pressure distributions obtained from the numerical analysis acting on the center of the bottom of the ground as shown in **Figure 4 (a)** are plotted. The x-axis represents the distance from the right edge of tunnel lining. The dotted line represents the initial vertical earth pressure before descending the trapdoor. In this figure, a decrease in vertical earth pressures acting on the trapdoor is observed, while the value above panel A increases with the descending of the trapdoor. Moreover, there is almost no change in the vertical pressure acting on panel B. When the FRSP was installed, the vertical pressure above the trapdoor becomes smaller. Therefore, it can be concluded that the effect of load dispersion is achieved. This effect is called an effect of load redistribution in this study. **Figure 7 (b)** shows the influence of the length of FRSP on the reduction ratio of the vertical load acting on the trapdoor. Y-axis represents the reduction of the vertical load acting on the trapdoor compare with the case of without FRSP. As observed from both numerical and experimental results, the FRSP can exert the effect of load redistribution when it is longer than 100 mm and this effect becomes more significant when the length of the FRSP increased.

The shear strain distribution for the cases without FRSP and with 200 mm long FRSP installed is plotted in **Figure 8**. The dotted line is the contour line which the shear strain is 2 %. When no FRSP was installed, the large shear strain concentrates on the edge of the trapdoor and develops towards the surface. Moreover, the large shear strain are concentrated in the belt-like region, that outlined by contour line as shown in **Figure 8**. The boundary of the large shear strain can be thought of as a slip line that generated due to the descending of the trapdoor. From the figure, it can be seen that the distance from the right edge of the lining

to the slip line is about 100 mm. When the FRSP was installed, the shear strain is intercepted by the piles, thereby making the shear strain above the piles become smaller. This effect is referred to as the effect of shear reinforcement.

Figure 9 shows the bending moment and the axial force distribution for different lengths of the FRSP. The difference in the line shape represents the different trends of the bending behavior. X-axis represents the length of the horizontal distance from the right edge of tunnel lining model. Each curve has different length in the x-axis direction due to the difference in length of FRSP. It is observed from **Figure 9 (a)** that upper side is tensioned when the FRSPs are shorter than 120 mm (plotted in heavy line). When the FRSP are longer than 120 mm, on the boundary of point M which is 100 mm away from lining model, the upper side of the FRSP is tensioned between OM, and the lower side of the FRSP is tensioned between MN. In addition, the maximum bending moment of MN part becomes larger, with the increase in pile length and there is almost no change when the length is longer than 260 mm (plotted in dot-line). This result shows the same trend with the reduction ratio of both the surface settlement and the vertical load. Bending moments have the value of zero around point M in all of the cases, which can be considered as the slip line goes past around the point M when the trapdoor is lowered.

The trend of the axial force distribution as shown in **Figure 9 (b)** indicates that the pile is tensioned when the FRSP is longer than 260 mm. This effect is due to the friction between the pile and the ground , which is named as the internal pressure effect in this study. Moreover, axial forces have increased when the FRSP become longer. Hence, the internal pressure effect becomes larger with the increase in the length of the FRSP.

3.2 Discussions of the experimental and the numerical results

The model experiments and the numerical analyses of the experiments were carried out to define clearly the effect of the FRSP on preventing the ground subsidence in a simple condition. The results show that the FRSP can prevent the surface settlement when it is longer than the distance from the lining model to the slip line and this effect becomes more significantly when the length of the FRSP increased. The advantages of the FRSP in the model experiment can be classified in to three categories as shown in **Figure 10** and described below.

First one is the effect of the shear reinforcement as shown in **Figure 10 (a)**. Based on the shear strain and the bending moment distributions as shown in **Figure 8 (a)** and **Figure 9 (a)** respectively, the distance from the lining model to the slip line is considered as 100 mm. On the other hand, when calculating the decreasing of the earth pressure, Terzaghi assumed that the shear line develops vertically to the surface from the edge of trapdoor as shown in **Figure11 (a)** (Terzaghi, 1943). Referring to the Terzaghi's assumption and numerical results, it is considered that the shear line generates same as AB curve as shown in **Figure11 (b)**. The distance from the lining model to the shear line is 100 mm in this experiment. When the FRSP is long enough to intersect with the slip line, it demonstrates the effect of the shear reinforcement for preventing the ground subsidence.

Second one is the effect of the load redistribution as shown in **Figure 10 (b).** From the vertical earth pressure distribution and bending moment of the FRSP, it can be considered that the FRSP can disperse the load acting on the trapdoor to the upper part of the Panel A. The vertical load acting on the trapdoor becomes smaller due to this mentioned effect, and as a result, the surface settlement will be decreased.

Third one is the effect of the internal pressure as shown in **Figure 10 (c)**. The tensile forces have occurred because of the friction between the FRSP and the surrounding ground, by which the ground will be reinforced. The settlement of the ground will be minimized due to the reinforcement of the ground.

4. Numerical analyses of a real construction case

4.1 Outline of numerical analysis of a real construction case

The mechanical behavior of the ground and the FRSP in the model experiment are considered to be different from real field condition. Hence, the results of the model experiment and the numerical analysis of the experiment are not sufficient to make clear the mechanism of the effect of the FRSP. Therefore, in this study two dimensional elasto-plastic FE analyses are performed to simulate a real tunnel excavation process to examine the mechanism of the effect of FRSP in an actual construction condition.

The analysis area and the boundary conditions are shown in **Figure 12**. This numerical object was determined based on the construction field data (Kitagawa et al., 2004). FE analysis code DBLEAVES (Ye et al., 2007) is also used in this analysis. *Subloading t_{ij} model,* which is utilized in the numerical analysis of

the model experiment, is also selected to simulate the ground material. The properties of the model ground are as given in **Table 3**.

The ground improvement as shown in **Figure 12** has been performed before the tunnel excavation, since the ground around tunnel was extremely soft with the *N* values smaller than 10. The ground in the improved area is modeled as an elastic material. Young's modulus was calculated from Eq. (1) and Eq. (2) (Japan Cement Association, 2007) based on the compressive strength q_u as shown in **Figure 12**.

$$N = \frac{q_u \times 8}{100} \tag{1}$$

$$E = 2800 \times N \ (kN/m^2) \tag{2}$$

The section of the tunnel lining is shown in **Figure 3**. The tunnel lining consists of the shotcrete and the tunnel support, hence it is modeled as a composite elastic beam, unifying the tunnel support and the shotcrete for convenience. The Young's Modulus of the composite elastic beam is taken as 1.23×10^7 kN/m^2. The hybrid element model which is used in the numerical analysis of the model experiment is also utilized for modeling the FRSP. The Young's Modulus of both the solid and the beam elements are 1.20×10^7 kN/m^2 and 1.90×10^8 kN/m^2 respectively.

4.2 Modeling of the tunnel excavation progress

In this study, tunnel excavation progress is simulated by the release of an equivalent in-situ stress due to excavation. Abovementioned objective tunnel where adopted the FRSP as the auxiliary tunneling methods, was constructed by an alternate excavation of the top heading and the bottom section. Therefore, both the top heading and bottom section excavation processes are simulated in the numerical analysis. The stress release rates of the top heading before installing the tunnel support and for the bottom section are determined as 40 % and 15 % respectively. The stress release rate was determined by setting the convergence of this analysis to be the same as the observed field data as plotted in the graph in **Figure 13**. Temporal change in the convergence and settlements of the tunnel when no FRSP was installed, including the numerical result and the observed field data are shown in **Figure 13**. It is observed from the figure, that these numerical data are identical to that observed from field data. This result indicates that the tunnel excavation process is simulated accurately and from the results it can be confirmed that the

abovementioned assumptions of the numerical analysis are appropriate.

4.3 Surface settlement under real construction condition

Temporal change in the settlements of the ground surface, foot and crown of the tunnel for the cases without a pile and with 1.00, 2.75, or 6.00 m long FRSP were installed are plotted in **Figure 14 (a)**. When the FRSP are installed, the settlement values become smaller and it can be concluded that the FRSP is effective on controlling the settlement of the ground surface and the tunnel. Reduction ratio of the settlement of the ground surface, crown and foot of the tunnel when the tunnel excavation was completed for different lengths of the FRSP are as shown in **Figure 14 (b)**. The figure indicates that the FRSP can prevent the settlement of the ground and the tunnel in all of the cases and it becomes more effective when the length of the FRSP is increased. In addition, the effect of the FRSP on preventing the settlements of the ground surface and the tunnel are increased rapidly when the FRSP are longer than 2.0 m and the graph reaches its peak at the length of 4 m.

4.4 Mechanical behavior of the ground under real construction condition

The vertical earth pressure distributions acting on the marked position (dotted line above the tunnel lining) when top heading excavation is completed are shown in **Figure 15 (a)**. The straight line shows the initial vertical load before the tunnel excavation. In the case with 2.75 m long FRSP was installed, the vertical earth pressure acting on the upper part of the tunnel becomes smaller when the vertical earth pressure acting on the upper part of the FRSP becomes larger. This result shows that the FRSP can disperse the load of the tunnel and the ground above the tunnel to the surrounding ground. This effect is also called as an effect of load redistribution. However, the effect of load redistribution could not observed in the case that 1.00 m long FRSP was installed.

The reduction ratio of vertical load acting on the marked position for different lengths of the FRSP is plotted in **Figure 15 (b)**. From the figure it can be observed that the FRSP demonstrates the redistribution effect when it is longer than 2.0 m. This is the possible cause of the following result that the effect of preventing the settlement of the tunnel and the ground increases at a great rate when the FRSP is longer than 2.0 m. However, for the cases with the FRSP shorter than 2.0 m was installed, the vertical load acting

on the upper part of the tunnel is larger than the case without a pile. The possible cause of this phenomenon can be as follows: when the FRSP is shorter than or equal to 2.0 m, it will interfere with the soil between the lining and the slip line, causing the rise in the load acting on the upper part of the tunnel.

The shear strain distributions when the top heading excavation is completed, are shown in **Figure 16**. The full line and the dotted line in this figure are the contour lines which the shear strain is 1% and 0.5 % respectively. When no FRSP was installed, a large shear strain is generated at the foot of the tunnel and it develops downward obliquely, then another large shear strain is generated from the edge of the improved ground and it develops upward vertically. For the cases where the 2.75 and 6.00 m long are installed, the shear strain generated form the edge of the improved ground is intercepted by the piles thereby making the shear strain around tunnel to become smaller. This effect is referred to as the effect of shear reinforcement, and it becomes more effective with the increase in the length. However, there is no significant effect when the length of FRSP was 1.0 m. Moreover, the FRSP has no effect on the shear strain generated from the foot of the tunnel.

4.5 Mechanical behavior of the FRSP under real construction condition

The bending moments of the FRSP when the tunnel excavation is completed are shown in **Figure 17**. As for the 1st piles which was installed during the top heading excavating progress, the upper side of the first pile is tensioned. On the other hand, the lower sides of piles are tensioned for the 2nd and 3rd piles which are installed during the excavating progress of the bottom section. The 1st piles work like a beam, which disperse the earth pressure acting on the tunnel lining to the ground on both sides of the tunnel. In addition, the bending moment occurring in the 1st piles are larger than the other piles. This result can be interpreted as the1st pile is more effective than other piles.

Figure 18 shows the axial force acting on the FRSP after the tunnel excavation has been completed. The1st and the 2nd FRSPs are tensioned and the tensile force is acting on the tunnel supports as an internal pressure. This internal pressure can restrain the deformation of the ground around the tunnel, thereby controlling the ground subsidence like rock bolts. This effect is called the effect of the internal pressure.

The bending moment and axial force distribution of the FRSP installed in the top heading for different lengths of the FRSP are shown in **Figure 19**. The bending moment distribution (**Figure 19 (a)**) indicates

that when the piles are shorter than or equal to 3.0 m, the upper side of the pile is tensioned and the maximum moment becomes larger when the length of the FRSP is increased. When the FRSP is longer than 3.0 m, the lower side of the pile is tensioned in the part that is at a distance from the tunnel lining, and there is almost no change when the FRSP is longer than 5.0 m. In addition, the distance from the lining to the position where the maximum moment occurs is about 2.0 m in all of the cases. The trend of the axial force distribution (**Figure 19(b))** is that the pile is tensioned in all of the cases independent of the length of the FRSP. This is due to the friction between the piles and the ground and this effect is named as internal pressure effect in this study. Moreover, the maximum axial force increases when the FRSP becomes longer. This trend implies that the internal pressure effect becomes more significantly when the length of the FRSP increases.

4.6 Discussion of the mechanism of the FRSP in real construction field

The numerical analysis results indicated that the FRSP can prevent the settlements of the ground and the tunnel effectively in real tunnel construction conditions. The advantages of the FRSP are presented as the three kinds of effects as shown in **Figure 20**, and described below:

First one is the effect of the shear reinforcement. From abovementioned numerical analysis results, the slip lines occurring in the ground due to the tunnel excavation can be concluded as shown in **Figure 20**. The slip line, which generated from the corner of the improved ground is 2.0 meters away from the tunnel lining, and the distance from the tunnel lining to the slip line is named as Q in this research work. When the length of the piles are longer than Q, the FRSP demonstrates the effect of shear reinforcement preventing the ground subsidence.

Second one is the effect of the load redistribution. When the FRSP is longer than Q that long enough to intersect with the slip line, it demonstrates a bending stiffness similar with a beam that distributes earth pressure over the tunnel lining to the surrounding ground.

Third one is the effect of the internal pressure. The FRSP demonstrates the effect of the internal pressure, which reinforces the ground around the tunnel in all of the cases. The settlement of the ground and the tunnel is prevented as a result of the reinforcement of the ground.

In addition, abovementioned three kinds of effects become more significantly, when the length of the

FRSP is increased. The relation between the lengths of the FRSP and the reduction ratio of the surface settlement obtained from the model experiment, the analysis of the model experiment and the real construction condition are shown in **Figure 21**. The x-axis represents the length of the FRSP, which is normalized with the distance from the lining model to the slip line Q. The Q of the model experiment and the real construction condition is 0.1 m and 2.0 m respectively. This figure indicates the FRSP exerts the effect to preventing the ground subsidence, when it is longer than Q. Moreover, this effect becomes more effective with the increase in the length of the FRSP and hits a peak, when the length is longer than 2.5 Q. As a summary, the rational length of the FRSP is between 1 Q to 2.5 Q, where Q is the distance from the lining to the slip line. Moreover, when the FRSP is shorter than 1 Q, the settlements will not be minimized, and when the FRSP is longer than 2.5 Q, it will become an excessive design.

Moreover, all of the experimental and the numerical results represent that , the distance from the lining model to the slip line Q is the extremely important parameter. Therefore, in the design and the construction of a FRSP, the most important issue to be considered is the estimation of the location of slip line. **Figure 22** shows the location of the slip line (Japan Society of Civil Engineers, 2007) during the calculation of the loosening earth pressure. The slip line generated by the tunnel excavation can be estimated easily by using this assumption. However, this method is limited to the homogeneous ground condition. Moreover, the non-uniform ground condition is faced more frequently in the real field, thus FE analysis can be used for these conditions.

5. Conclusions

In this paper, three dimensional trapdoor model experiments and the corresponding numerical analyses, and numerical analyses for the actual tunnel construction are carried out to make clear the mechanism of the effect of FRSP on preventing settlements of tunnel and surrounding ground.

The experimental and numerical results indicate that, the FRSP can prevent the settlements of the ground surface and the tunnel effectively. The advantage of the FRSP can be categorized as the effect of the shear reinforcement, load redistribution, and internal pressure. FRSP can exert the effect of shear reinforcement and load redistribution, when it is longer than the distance from the tunnel lining to the slip line. On the

other hand, FRSP can exert the effect of internal pressure independent of the length of FRSP. Moreover, these 3 kinds of effects are become more significantly, when the length of FRSP is increased.

References

Adachia, T., Kimura, M., Kishida, K., 2003. Experimental study on the distribution of earth pressure and surface settlement through three-dimensional trapdoor tests, Tunnelling and Underground Space Technology, 18 (2-3), pp. 171-183. Doi: 10.1016/S0886-7798(03)00025-7

Adachi, T., Tamura, T., Yahima, A. and Ueno, H., 1986. Surface subsidence above shallow sandy ground tunnel, JSCE Journal of Geotechnical Engineering, 370 (III-5), 85-94. Doi: doi.org/10.2208/jscej.1986.370_85

Akutagawa., S., Lee, J., Doba, N., Kitagawa, T., Isogai, A. and Matsunaga, T., 2006. Identification and prediction of deformation behavior around a shallow NATM tunnel using strain softening model, Tunnelling and Underground Space Technology 21, 387. Doi: 10.1016/j.tust.2005.12.198

Cui, Y., Kishida, K. and Kimura, M., 2007. Experimental study on effect of auxiliary methods for simultaneous settlement at subsurface and surface during shallow overburden tunnel excavation, Japanese Geotechnical Journal, 3(3), 261-272. (in Japanese) Doi: doi.org/10.3208/jgs.3.261

Fang, Q., Zhang, D. and Wong, Y. N.L., 2012. Shallow tunnelling method (STM) for subway station construction in soft ground, Tunnelling and Underground Space Technology, Vol. 29, pp.10-30. Doi: 10.1016/j.tust.2011.12.007

Fukushima, S., Mochizuki, Y., Kagawa, K. and Yokoyama, A., 1989. Model test on prereinforcement of shallow tunnel in sandy ground, Doboku Gakkai Ronbunshu, JSCE, 2010(406), 79-86. (in Japanese) Doi: doi.org/10.2208/jscej.1989.406_79

Iizuka, A. and Ohta, H., 1987. A determination procedure of input parameters in elasto-viscoplastic finite element analysis, Soils and Foundations, 27(3), 71-87. Doi: doi.org/10.3208/sandf1972.27.3_71

Japan Society of Civil Engineers, 2007. Standard specifications for tunneling-2006: shield tunnels, Maruzen Co. Ltd., Tokyo. ISBN: 978-4-8106-0568-6

Japan Cement Association, 2007. Manual of ground improvement using cementitious material, Gihodo Shuppan Co. Ltd, Tokyo. (in Japanese) ISBN:9784765516556

Karakus, M. and Fowell, R.J., 2003. Effects of different tunnel face advance excavation on the settlement by FEM, Tunnelling and Underground Space Technology, 18, 513-523. Doi: 10.1016/S0886-7798(03)00068-3

Kikumoto, M., Kimura, M., Kishida, K. and Adachi, T., 2003. Three dimensional trapdoor experiments and its numerical analysis on the mechanical behavior during tunnel excavation, Doboku Gakkai Ronbunshu, JSCE, 2003(750), 145-158. DOI: 10.2208/jscej.2003.750_145

Kitagawa, T., Goto, M., Tamura, T., Kimura, M., Kishida, K., Cui, Y., Yashiro, K., 2009. Experimental studies on tunnel settlement reduction effect of side piles, Doboku Gakkai Ronbunshuu F, JSCE, 65(1), 73-83. DOI: 10.2208/jscejf.65.73

Kitagawa, T., Goto, M., Tamura, T., Kimura, M., Kishida, K., Yashiro, K., Shimamoto, K., 2010. Numerical analyses of tunnel settlement reduction effect by side piles, Doboku Gakkai Ronbunshuu F, JSCE, 66(1), 85-100. DOI: 10.2208/jscejf.66.85

Kitagawa, T., Isogai, A., Okutsu, K., Kawaguchi, T., 2004. Excavation through earth ground with small burden by soil improvement and side pile – ushikagi Tunnel on Tohoku Shinkansen line, Tunnels and Underground, JTA, 35(4), 255-262, 2004. (in Japanese)

Mair, R. J., Taylor, R. N. and Bracegirdle, A., 1993. Subsurface settlement profiles above tunnel in clays, Geotechnique, 43 (2), 315-320. DOI: 10.1016/0148-9062(93)91702-K

Miwa, M. and Ogasawara, M., 2005. Tunnelling through an embankment using all ground fasten method, Tunnelling and Underground Space Technology, 20(2), 121-127, 2005. DOI: 10.1016/j.tust.2003.12.001

Murayama, S. and Matsuoka, H., 1971. Earth pressure on tunnel in sandy ground, Proceedings of the Japan Society of Civil Engineers, 1971(187), 95-108. (in Japanese) Doi.org/10.2208/jscej1969.1971.187_95

Irshad, M., Heflin, L. H., 1988. Soft-ground NATM tunnel designs for the Washington, D.C. Metro, Tunnelling and Underground Space Technology, 3(4), 385-392. Doi: 10.1016/0886-7798(88)90010-7

Nakai, T. and Hinokio, M., 2004. A simple elastoplastic model for normally and over consolidated soils with unified material parameters, Soils and Foundations, 44 (2), 53-70. Doi: 10.3208/sandf.44.2_53

Nakai, T., Xu, L. M. and Yamazaki, H., 1997. 3D and 2D Model Tests and Numerical Analyses of Settlements and Earth Pressures due to Tunnel Excavation, Soils and Foundations, 37 (3), 31-42. Doi: 10.3208/sandf.37.3_31

Ocak, I., 2008. Control of surface settlement with umbrella arch method in second stage excavations of Istanbul Metro, Tunnelling and Underground Space Technology, 23, 674-681. Doi: 10.1016/j.tust.2007.12.005

Okawa, T., Yokoyama, J., Ishihara, H. and Kojima, W., 1985. Effect of pipe-roof in tunnelling method, Doboku Gakkai Ronbunshu, 355(VI-2), 100-107. (in Japanese) Doi: 10.2208/jscej.1985.355_100

Pinto, F., Zymnis, D., and Whittle, A., 2013. Ground movements due to shallow tunnels in soft ground. II: Analytical Interpretation and Prediction, Journal of geotechnical and geoenvironmental engineering, ASCE, 140(4), 04013041. Doi: 10.1061/(ASCE)GT.1943-5606.0000947.

Shimada, T., 1980. Surface Settlement above the conventionally excavated tunnels with thin earth cover, Proceedings of the Japan Society of Civil Engineers, 296, 97-109. (in Japanese) Doi: 10.2208/jscej1969.1980.296_97

Akutagawa, S., Lee, J.-H., Doba, N., Kitagawa, T., Isogai, A. and Matsunaga, T., 2006. Identification and prediction of deformation behavior around a shallow NATM tunnel using strain softening model, Tunnelling and underground Space Technology, 21(3), 387. Doi: 10.1016/j.tust.2005.12.198

Terzaghi, K., 1943. Theoretical Soil Mechanics, John Wiley & Sons, New York. Doi: 10.1002/9780470172766

Ye, B., Ye, G. L., Zhang, F. and Yashima, A., 2007. Experiment and numerical simulation of repeated liquefaction-consolidation of sand, Soils and Foundations, 47 (3), 547-558. Doi: 10.3208/sandf.47.547

Yokoyama, A., Horiuchi, Y. and Kimura, K., 1987. Settlement behavior of sandy ground above shallow tunnels, Doboku Gakkai Ronbunshu, 1987(388), 151-160. (in Japanese) Doi: 10.2208/jscej.1987.388_151

Yoo, C., Shin, H.K., 2003. Deformation behavior of tunnel face reinforced with longitudinal pipes−laboratory and numerical investigation, Tunnelling and Underground Space Technology, 18, 303-319. Doi: 10.1016/S0886-7798(02)00101-3

Zhang, F., Kimura, M., Nakai, T. and Hoshikawa, T., 2000. Mechanical behavior of pile foundations subjected to cyclic lateral loading up to the ultimate state, Soils and Foundations, 40 (5), 1-17. Doi: 10.3208/sandf.40.5_1

Table 1. Properties of the Toyoura silica sand and the model ground

Specific gravity G_s	2.64
Unit weight γ [kN/m^3]	15.5
Void ratio e	0.627
Maximum void ratio e_{max}	0.982
Minimum void ratio e_{min}	0.580
Relative density D_r [%]	88.3

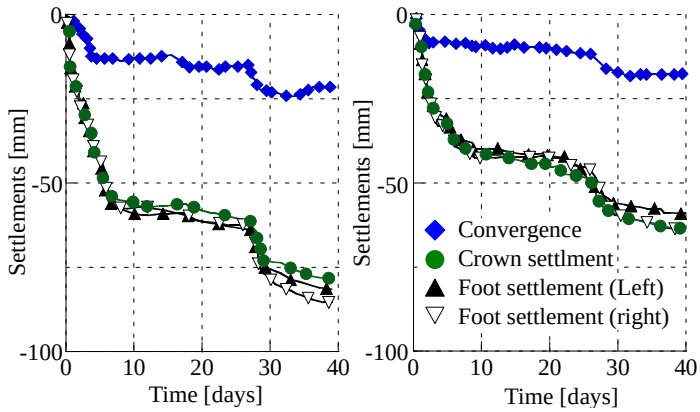

(a) No FRSP (b) With FRSP

Figure 1. Temporal change in the settlements of the tunnel and the convergence (Ushikagi Tunnel)

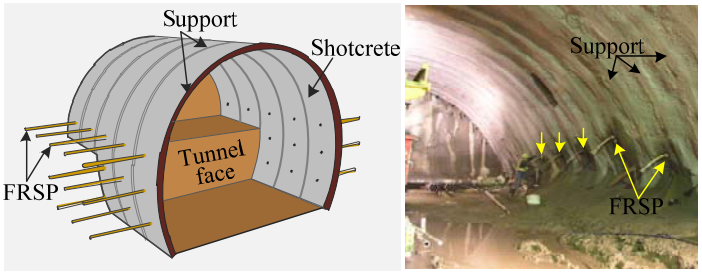

Figure 2. Foot reinforcement side pile

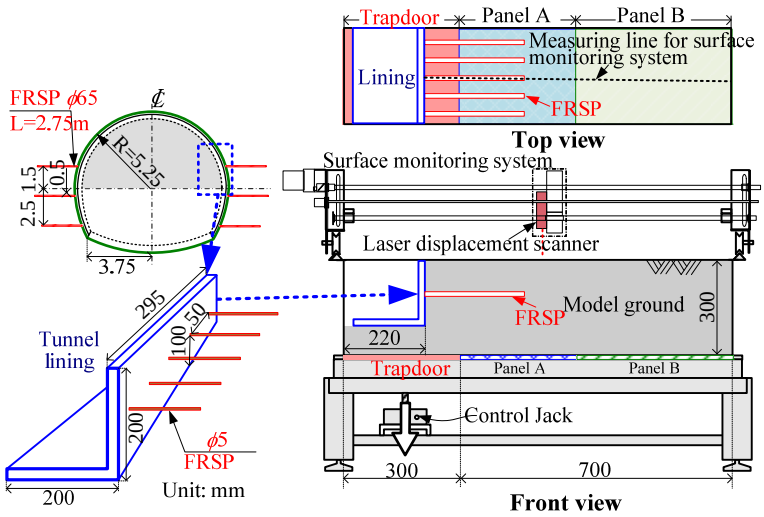

Figure 3. Three dimensional trap door apparatus

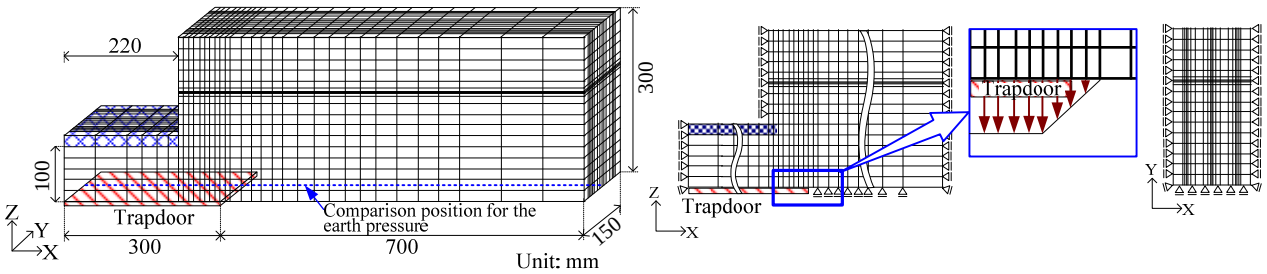

(a) Mesh of numerical analysis area (b) Boundary and loading conditions

Figure 4. Mesh and the boundary conditions of the numerical analysis of model experiment

Table 2. Parameters used in the numerical analyses of model experiments (Cui et al., 2007)

Specific gravity G_s	2.64
Unit weight γ [kN/m^3]	15.5
Void ratio e	0.627
Poisson's ratio ν	0.33
principal stress ratio at critical state M_f	1.506
compression index λ	0.07
swelling index κ	0.0045
shape of yield surface β	2.0
influence of density and confining pressure a	500

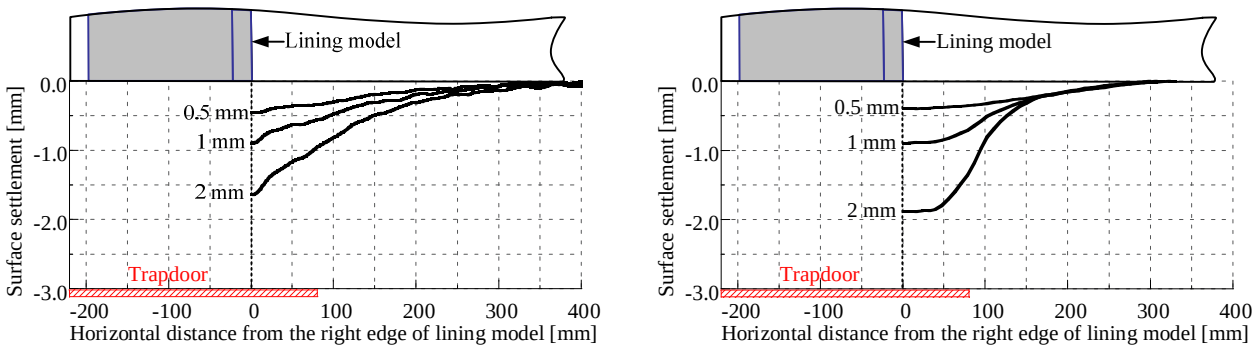

(a) Experimental result (b) Numerical result

Figure 5. Comparison of the experimental and the numerical results

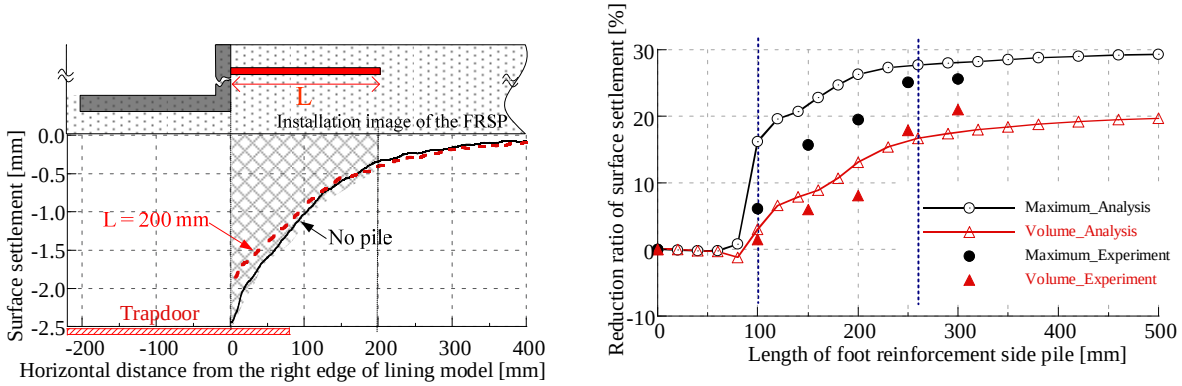

(a) Effect of the FRSP on Surface Settlement (Experimental result) (b) Influence of the length of the FRSP

Figure 6. Influence of the length of the FRSP on surface settlement

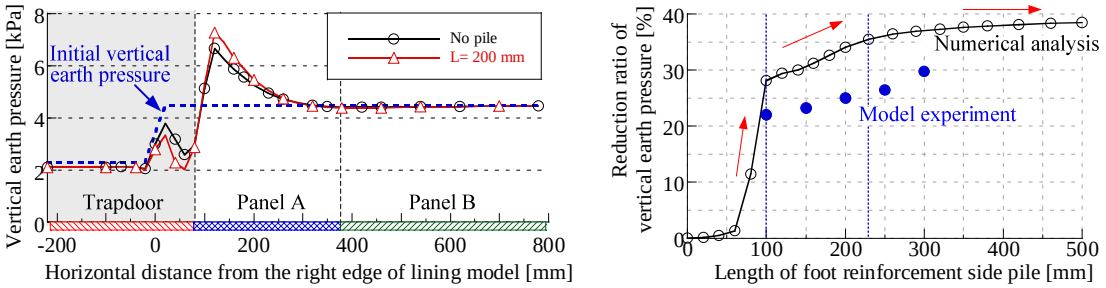

(a) Vertical earth pressure distributions (b) Influence of the length of the FRSP on vertical load

Figure 7. Influence of the length of the FRSP on vertical load (Numerical result)

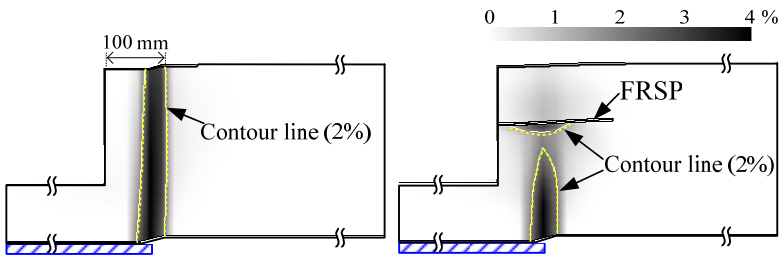

(a) No FRSP (b) With FRSP (L=200 mm)

Figure 8. Shear strain distribution (Numerical result)

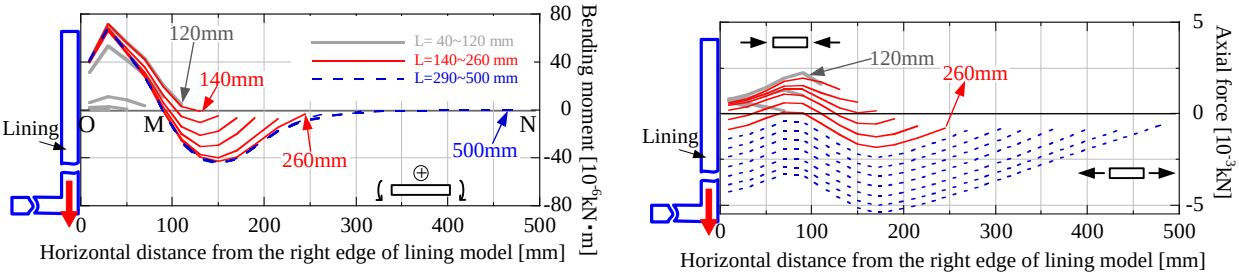

(a) Bending moment distribution (b) Axial force distribution

Figure 9. Mechanical behavior of the FRSP in the model experiment (Numerical result)

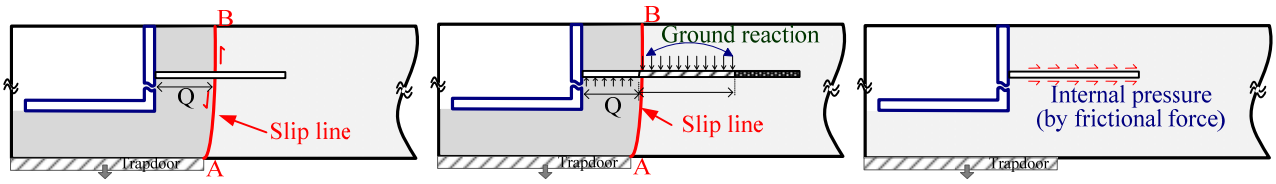

(a) Shear reinforcement (b) Load redistribution (c) Internal pressure

Figure 10. Mechanism of the effect of the FRSP in the model experiment

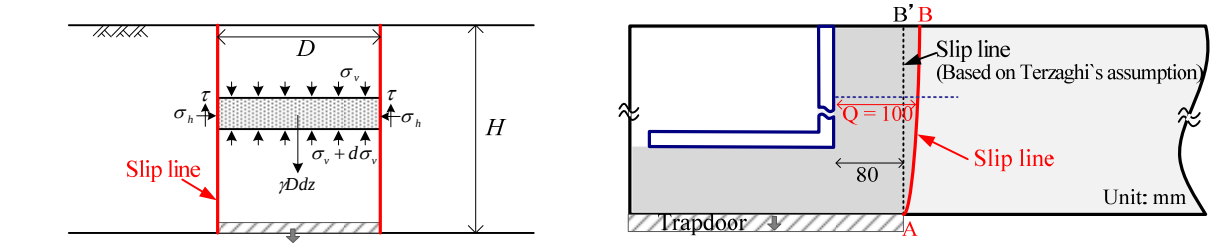

(a) Earth pressure around the trapdoor proposed by Terzaghi (1943) (b) Slip line of the model experiment

Figure 11. Slip line occurring due to lowering of the trapdoor

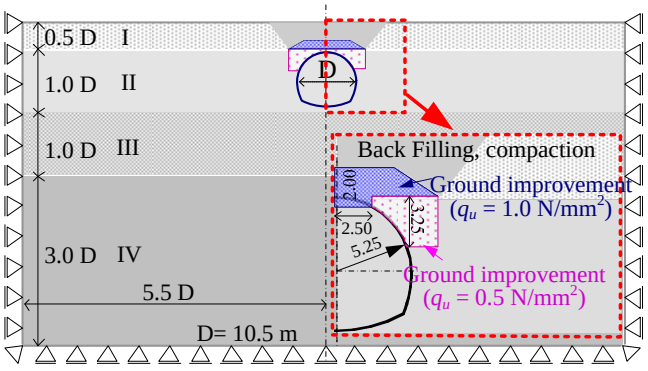

Figure 12. Numerical model of the real construction condition

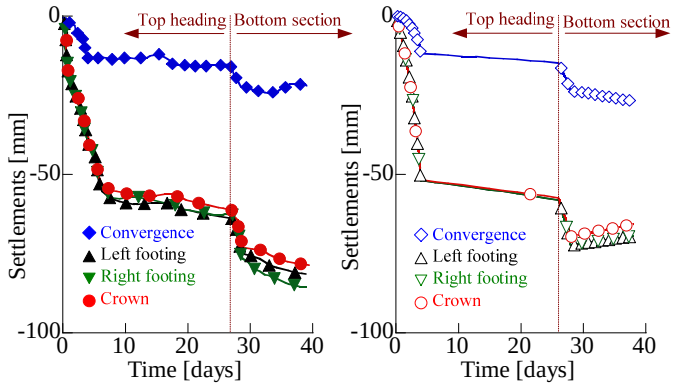

(a) Observed field data (b) Numerical results

Figure 13. Comparison of the field data with the numerical results

(Without FRSP)

Table 3. Properties of the ground in the real construction condition

	I	II	III	IV	Backfill
Density (10^3kg/m^3)	1.609	1.805	1.832	1.550	1.609
Poisson's ratio (ν)	0.360	0.360	0.290	0.290	0.261
Void ratio (e_0)	1.704	1.071	1.012	0.613	0.852
Coefficient of earth pressure at rest k_0	0.562	0.562	0.409	0.409	0.353
Principal stress ratio at critical state R_{cs}	2.550	2.550	3.888	3.888	4.668
Compression index λ	0.137	0.070	0.070	0.082	0.094
Swelling index κ	0.030	0.005	0.005	0.018	0.021

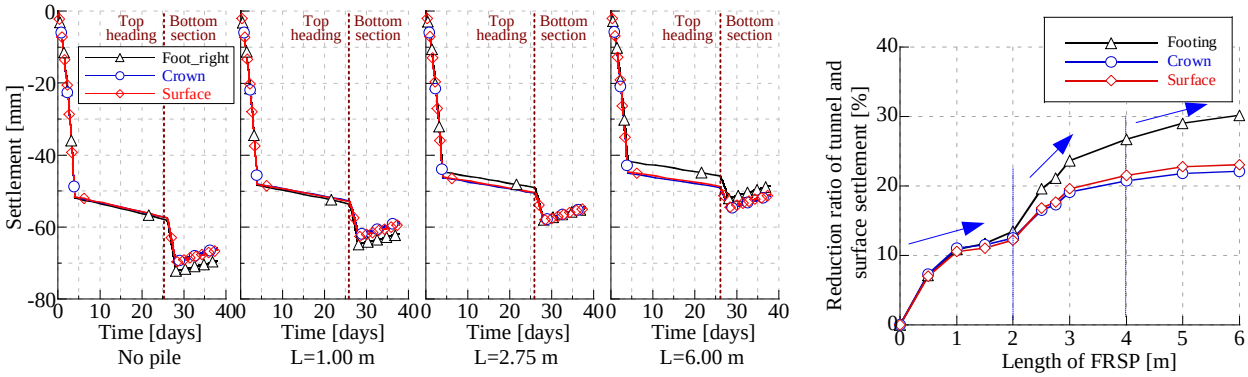

(a) Variation of settlements of ground surface and tunnel (b) Influence of the length of FRSP

Figure 14. Effect of the FRSP on the settlements in the real tunnel construction

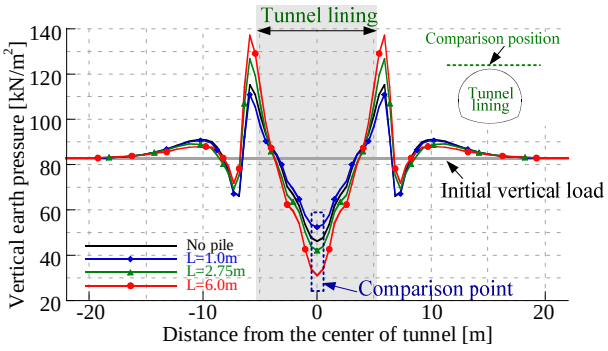

(a) Vertical load distribution

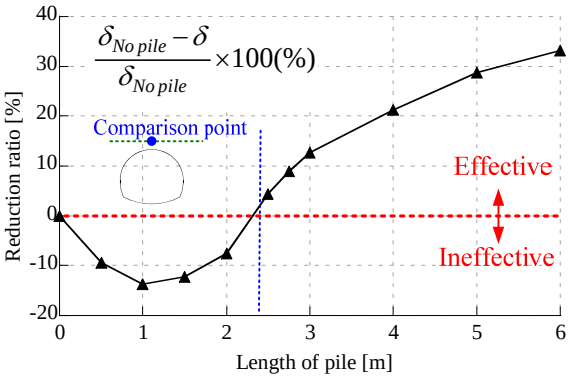

(b) Influence of the length of FRSP on vertical load

Figure 15. Effect of the FRSP on the vertical load distribution in real tunnel construction

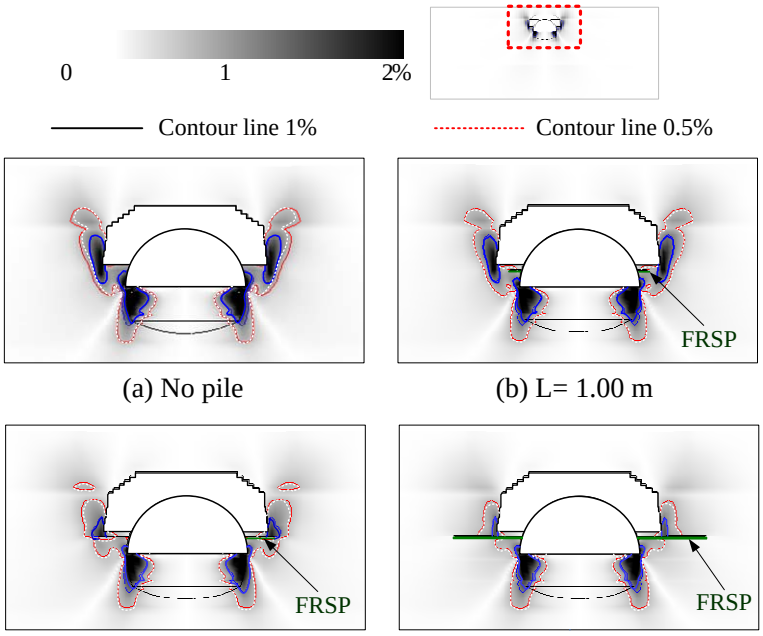

(a) No pile (b) L= 1.00 m

(c) L= 2.75 m (d) L=6.00 m

Figure 16. Shear strain distribution in real tunnel construction

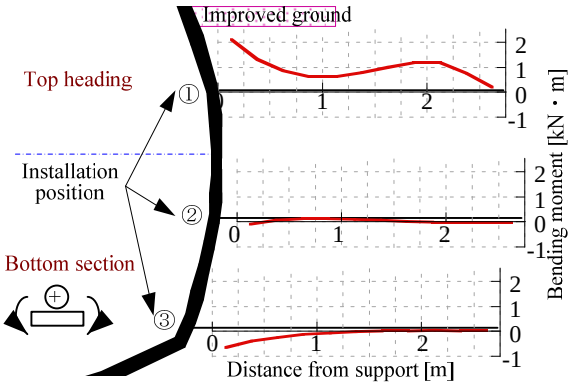

Figure 17. Bending moment distribution (L=2.75 m)

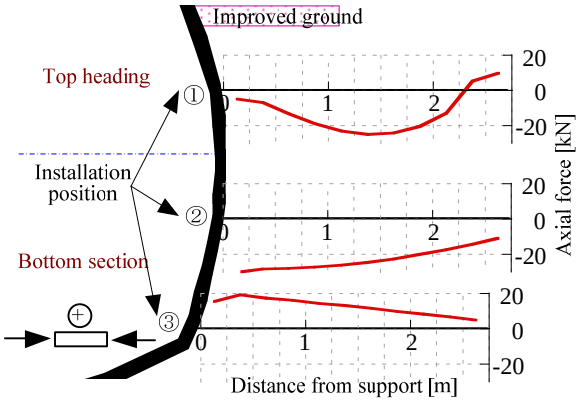

Figure 18. Axial force distribution (L=2.75 m)

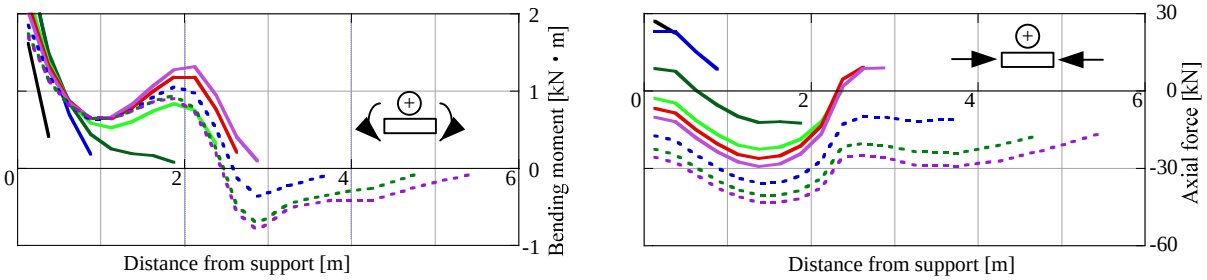

(a) Bending moment distribution (b) Axial force distribution

Figure19. Mechanical behavior of FRSP in real tunnel construction (Installed in top heading)

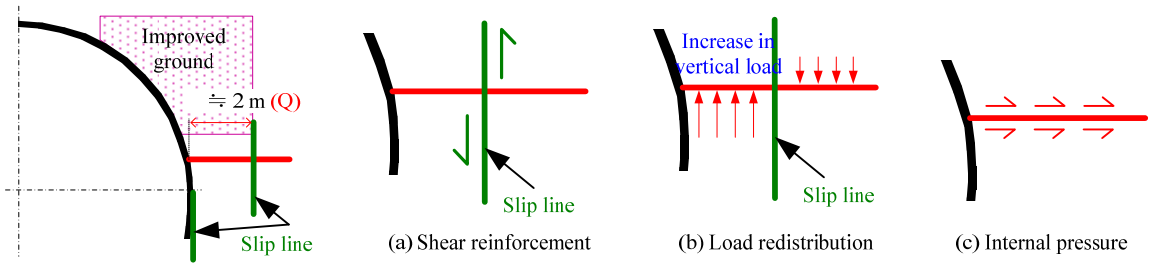

Figure 20. Mechanism of the effect of the FRSP in real tunnel construction

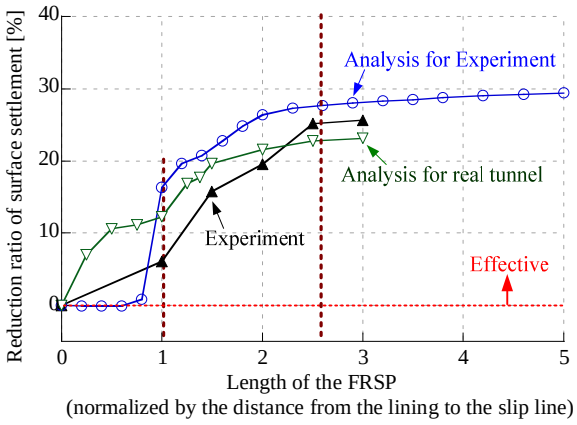

Figure 21. Influence of the length of the FRSP on the reduction ratio of surface settlement

(Normalized by the distance from the lining to the slip line)

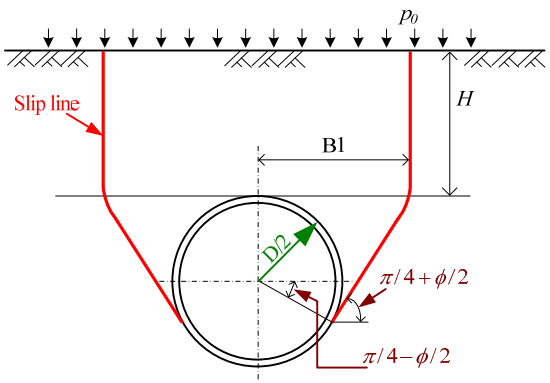

Figure 22. Loosening earth pressure due to the tunnel

excavation proposed by Terzaghi (Terzaghi, 1943)